

# Scaling and Interference in the Dissociation of Halo Nuclei

M. S. Hussein, R. Lichtenthaler,

*Instituto de Fisica, Universidade de Sao Paulo, C.P. 55318, 05315-970, Sao Paulo, SP, Brazil*

F. Nunes,

*National Superconducting Cyclotron Laboratory, Michigan State University, East Lansing, Michigan 48824-1321*

and I.J. Thompson

*Physics Department, University of Surrey, Guildford, Surrey, GU2 7XH, U.K.*

(Dated: July 12, 2018)

The dissociation of halo nuclei through their collision with light and heavy targets is considered within the Continuum Discretized Coupled Channels theory. We study the one-proton halo nucleus  $^8\text{B}$  and the one-neutron halo nucleus  $^{11}\text{Be}$ , as well as the more normal  $^7\text{Be}$ . The procedure previously employed to extract the Coulomb dissociation cross section by subtracting the nuclear one is critically assessed, and the scaling law usually assumed for the target mass dependence of the nuclear breakup cross section is also tested. It is found that the nuclear breakup cross section for these very loosely bound nuclei does indeed behave as  $a + bA^{1/3}$ . However, it does not have the geometrically inspired form of a circular ring which seems to be the case for normal nuclei such as  $^7\text{Be}$ . We find further that we cannot ignore Coulomb-nuclear interference effects, which may be constructive or destructive in nature, and so the errors in previously extracted  $B(E1)$  using the subtraction procedure are almost certainly underestimated.

PACS numbers: 25.60.Dz, 25.70.De, 24.10.Eq

The study of electromagnetic dissociation of halo nuclei is an important area that supplies invaluable information about their multipole responses and consequently the details of their structure [1, 2]. The theory usually employed for the purpose is the relativistic Coulomb excitation theory developed by Winther and Alder [1, 3] which hinges on the Fermi-Weisacker-Williams (FWW) virtual photon method. Since the measurement of the dissociation cross section supplies the combined Coulomb and nuclear contributions, one is forced to subtract the latter. The common prescription employed for this subtraction procedure is the so-called scaling law: the nuclear breakup cross section should scale linearly with the radius of the target, and thus by measuring the cross section for the breakup of the halo nucleus in the predominantly nuclear field of a light target, one attempts to extrapolate to heavy targets assuming the validity of the scaling law. The Coulomb dissociation cross section for the halo nucleus on the heavy target is then simply obtained by subtracting from the experimental cross section an extrapolated nuclear one calculated according to some prescription. It is this “nuclear-free” cross section which is fitted by the FWW result in order to extract the  $B(EL)$  distribution [4, 5, 6, 7, 8, 9, 10, 11, 12, 13, 14, 15, 16, 17].

Two factors convinced us to critically assess this procedure. Several theorists [18, 19, 20, 21, 22, 23] have recently cast doubt on the relative importance of the nuclear contribution to the dissociation cross section, claiming in some cases that this contribution can be significantly larger than the Coulomb contribution in as heavy a target as lead, invalidating the scaling law. The second important factor is the need to supply a quantitative assessment of the Coulomb-nuclear interference terms in

the cross section.

The purpose of this letter is to settle these issues by performing a full Continuum Discretized Coupled Channels calculation for  $^8\text{B}$ ,  $^{11}\text{Be}$  and  $^7\text{Be}$  dissociations in the fields of light-, medium- and heavy-mass targets at three laboratory energies where data are available.

Coupled channels calculations were therefore performed to calculate the elastic breakup (also called diffraction dissociation) arising in a three-body model consisting of a two-body projectile incident on an inert target [24, 25]. Between the target and each of the two projectile components we specify optical potentials whose imaginary parts describe the loss of flux to channels beyond elastic breakup. We calculate all orders of the tidal effects of the optical potentials as they deform and break up the projectile.

For both  $^8\text{B}$  and  $^{11}\text{Be}$ , projectile states were included for relative motion up to partial waves  $\ell_{\text{max}} = 3$  and energy  $\epsilon_{\text{max}} = 10$  MeV. This energy range was divided into 20 bins when  $\ell = 0$  for  $^8\text{B}$  and when  $\ell = 0, 1$  for  $^{11}\text{Be}$ . There were 10 bins when  $\ell = 1, 2$  for  $^8\text{B}$  and  $\ell = 2$  for  $^{11}\text{Be}$ , and 5 bins in the remaining partial waves, all evenly spaced in momentum  $k$ . The coupled channels for the scattering of the projectile on the target were solved up to  $R_{\text{max}} = 500$  fm, and for partial waves up to  $KR_{\text{max}}$  where  $K$  is the wave number for the incident beam. The optical potentials have the same parameters for all energies, as given in Table I, using radii calculated with an  $A^{1/3}$  contribution from the target mass number. We thus impose a regular target scaling in the radial geometry of the component-target potentials, in order to examine the contributions from varying target size and varying dynamical conditions.

TABLE I: Optical and binding potential parameters for  $^8\text{B}$  and  $^{11}\text{Be}$  projectiles.

Pair	$V$	$r_0$	$a$	$W$	$r_i$	$a_i$
	MeV	fm	fm	MeV	fm	fm
p+T	46.979	1.17	0.75	6.98	1.32	0.60
$^7\text{Be}$ +T	114.2	1.0	0.85	9.44	1.30	0.81
n+T	37.14	1.17	0.75	8.12	1.26	0.58
$^{10}\text{Be}$ +T	46.92	1.204	0.53	23.5	1.33	0.53
n+ $^{10}\text{Be}$ s	51.51	1.39	0.52			
partial waves <i>pdf</i>	28.38	1.39	0.52	$V_{so}$	$r_{so}$	$a_{so}$
p+ $^7\text{Be}$	44.675	1.25	0.52	4.9	1.25	0.52

The results of the integrated nuclear breakup cross sections obtained from the CDCC calculations are shown in figure 1: circles and squares for  $^8\text{B}$  at  $E_{lab} = 44$  and 70 MeV/n respectively, left-triangle, down-triangle and right triangle for  $^{11}\text{Be}$  at  $E_{lab} = 44, 70,$  and 200 MeV/n respectively, and full diamonds for  $^7\text{Be}$  at 100 MeV/n (after [26]). These are plotted as functions of the cubic root of the mass of the target nucleus, proportional to the target's radius. They are all rather accurately accounted by a linear dependence on  $A_T^{1/3}$ , but with varying coefficients. We might expect that the total direct reaction cross-section is proportional to the area of a circular ring given [27] by:

$$\sigma_D \approx 2\pi a(R_P + R_T) \quad (1)$$

where  $a$  is approximately the diffuseness of the optical potential that describes the elastic scattering, and  $R_P + R_T$  is the sum of the projectile and target radii. In [27], it was found the Eq. (1) describes the data quite well. Guided by Eq. (1) we anticipate the following form of the nuclear breakup cross-section:

$$\sigma_N = P_1 + P_2 A_T^{1/3} \quad (2)$$

where the parameters  $P_1$  and  $P_2$  depend on the projectile, and may also depend on the bombarding energy and the structure of the target. We performed linear fits to the nuclear breakup cross sections as a function of  $A_T^{1/3}$  to obtain the values for  $P_1$  and  $P_2$  shown in the legends of Figs. 1.

The nuclear breakup cross section calculated with CDCC for  $^8\text{B}$  and  $^{11}\text{Be}$  do show the  $A_T^{1/3}$  dependence of Eq. (2) as seen in figures 1 but do not always follow the form given by Eq. (1), in particular as, in most cases, the cross section fits have  $P_1 < 0$ . At this point we should mention that our results disagree completely with those of [20], where the nuclear breakup cross section was found to scale as  $A_T$ . (In fact such a behaviour could only be possibly true for a very weakly interacting system where the whole volume of the target could be effective.)

This is not the case for  $^7\text{Be}$ , a normal non-halo nucleus, where scaling holds and Eq. (1) is fully satisfied, where both  $P_1$  and  $P_2$  are positive as seen in figure 1. The different behaviour in the scaling of the nuclear breakup

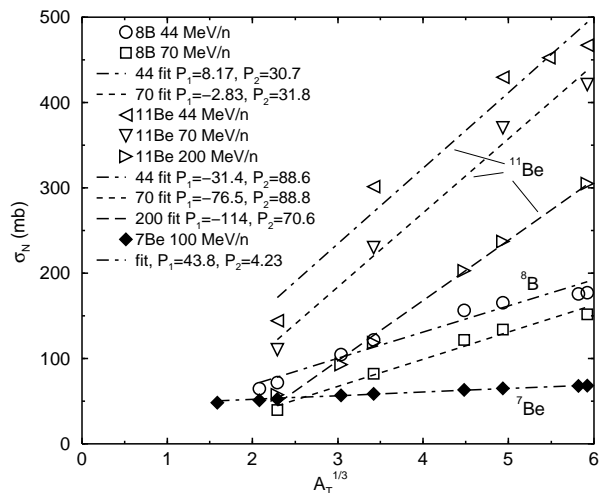


FIG. 1: Elastic nuclear breakup cross-section for  $^8\text{B}$ ,  $^{11}\text{Be}$  and  $^7\text{Be}$  projectiles at the indicated energies, as a function of target mass number  $A_T$ , along with linear fits.

cross-sections for  $^8\text{B}$  and  $^{11}\text{Be}$  could well be a manifestation of their halo nature.

The fact that the nuclear cross sections do not exactly satisfy Eq. (1) with  $P_1$  proportional to the radius of the projectile leads us to conclude that nuclear breakup must be estimated from realistic dynamical models, not from Eq. (1). As well as the present CDCC model, Glauber few-body procedures can be used, as done in refs. [28, 29, 30].

The analysis of experimental data [28, 29, 30] started with the following expression for the breakup cross section:

$$\frac{d\sigma}{dE^*} = S \frac{d\sigma_C}{dE^*} + L(A_T) \frac{d\sigma(^{12}\text{C})}{dE^*}, \quad (3)$$

where  $S$  is the ground state spectroscopic factor,  $E^*$  is the excitation energy. The  $d\sigma_C/dE^*$  is from the Coulomb FWW virtual photon formula, and the  $d\sigma(^{12}\text{C})/dE^*$  is what is observed for a  $^{12}\text{C}$  target. The  $L(A_T)$  is a scaling factor, which may be determined either by fitting Eq. (3) to the data, exploiting the different shapes of the excitation spectra, or by calculating

$$L(A_T) = \sigma_N^{\text{th}}(A_T) / \sigma_N^{\text{th}}(12) \quad (4)$$

using eikonal calculations of nuclear breakup  $\sigma_N^{\text{th}}(A_T)$ . The  $^{12}\text{C}$  is simply a reference nucleus. Of course the above incoherent sum ignores completely Coulomb-nuclear interference effects, which we discuss further below.

In [28, 29] the reaction  $^{11}\text{Be} + ^{208}\text{Pb}$  at  $E = 520$  MeV/n is considered. By adjusting  $S$  and  $L$ , these authors obtain  $L(208) = 5.6 \pm 0.4$ . This is close to our value of  $L$ , which can be extracted from Fig. 1 at  $E = 200$  MeV/n, namely  $L = 5.9$ . Our results also agree with the eikonal calculations of [31]. In fact, at  $E = 200$  MeV/n, it has been further confirmed to us [32] that within the

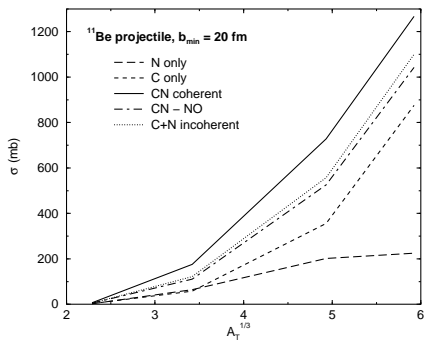


FIG. 2: Total breakup, Coulomb only, and nuclear only contributions for  $^{11}\text{Be}$  projectile as a function of  $A_T^{1/3}$ , for a lower radial cutoff  $b_{\min} = 20$  fm.

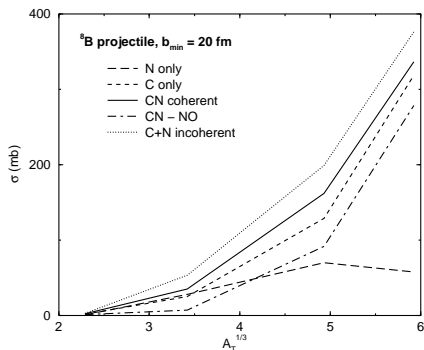


FIG. 3: Total breakup, Coulomb only cross-section and nuclear only breakup cross-section for  $^8\text{B}$  projectile, for a lower radial cutoff  $b_{\min} = 20$  fm.

eikonal formalism of [31], the value of  $L$  comes out about 5.5, very close to our model result.

On the other hand, using the same incoherent cross-section formulae, Ref. [30] analyses the reaction  $^{11}\text{Be} + ^{208}\text{Pb}$  at  $E = 70$  MeV. These authors found for  $L$  the value  $2.1 \pm 0.5$ , much smaller than our result  $L = 3.82$  (Fig. 1) but in accordance with the geometrical value obtained from Eq. (1), which we have shown to be not valid for halo nuclei for at least some halo nuclei. It is conceivable that the reason for this discrepancy resides in the neglect of the interference terms, which, as we see next, can be rather large.

The Coulomb and nuclear potentials combine together coherently to give breakup, and the destructive interference between these potentials in the surface region is well known. If, however, the nuclear and Coulomb breakup cross sections contribute largely to different partial waves, then the total breakup cross sections will add incoherently and Eq. (3) should be accurate.

In order to answer this question definitively at least in our test cases, we have performed further CDCC breakup calculations with both Coulomb and nuclear transition potentials as in [33, 34], along with sufficient radial and partial wave limits to encompass all the resulting breakup cross sections. For reference we also performed ‘Coulomb

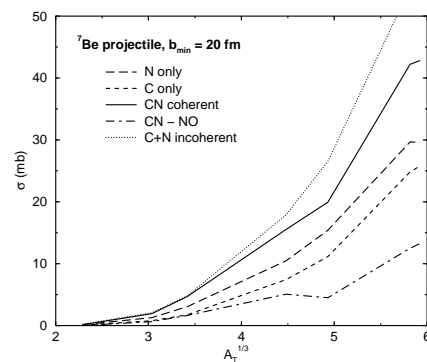


FIG. 4: Total breakup, Coulomb only and nuclear only breakup cross-section for  $^7\text{Be}$  projectile

only’ calculations, where there are no nuclear potentials at all. Any pure Coulomb calculation needs at least to be limited by a minimum impact parameter  $b_{\min}$  to simulate the effects of nuclear absorption during grazing and closer collisions.

The combined Coulomb and breakup calculation will therefore give a total

$$\sigma_{CN} = \sigma_C + \sigma_N + \sigma_I \quad (5)$$

which defines an interference term  $\sigma_I$  by the difference with the sum of Coulomb-only and nuclear-only calculations. We have found that  $\sigma_I$  is sometimes negative (destructive interference), sometimes positive (constructive interference), and often large. Thus, although one can construct  $\sigma_N$  from some scaling model, the mere subtraction of it from the data would give a ‘contaminated’ Coulomb breakup cross-section:

$$\hat{\sigma}_C = \sigma_C + \sigma_I = \sigma_{CN} - \sigma_N. \quad (6)$$

The use of, say, the equivalent photon method as done in [4, 5] to extract the  $B(E1)$  distribution for  $^8\text{B}$  and  $^{11}\text{Be}$  or for that matter any other halo nucleus could be questionable if  $\sigma_I$  is large. To ascertain typical sizes of  $\sigma_I$ , we first show in figures 2, 3 and 4 the cross-sections,  $\sigma_C$ ,  $\sigma_N$  and  $\sigma_{CN}$  as the short dashed, long dashed and solid lines respectively, for the  $^{11}\text{Be}$  and  $^8\text{B}$  at  $E_{\text{lab}} = 44$  MeV/n, and  $^7\text{Be}$  at  $E_{\text{lab}} = 100$  MeV/n, using  $b_{\min} = 20$  fm in each case.

To see this, in Figs. 2 and 3, we plot as the dot-dashed line the values of  $\sigma_{CN} - \sigma_N$ , which should ‘ideally’ agree with  $\sigma_C$  as the short dashed line. We also plot as the dotted line the incoherent sum  $\sigma_C + \sigma_N$ , whose difference from the  $\sigma_{CN}$  solid line indicates the effects of interference. It is evident that, for large  $A_T$ , the interference term is destructive for  $^8\text{B}$  (the solid line  $\sigma_{CN} < \sigma_{C+N}$  dotted line), so its neglect may lead to unrealistically smaller  $B(E1)$  distributions. Conversely, it is constructive for  $^{11}\text{Be}$ , yielding an unrealistically larger  $B(E1)$ .

Experimentalists (e.g. [17]) often try to minimise these interference problems by restrictions to small excitation energies, and/or to large impact parameters. We focus

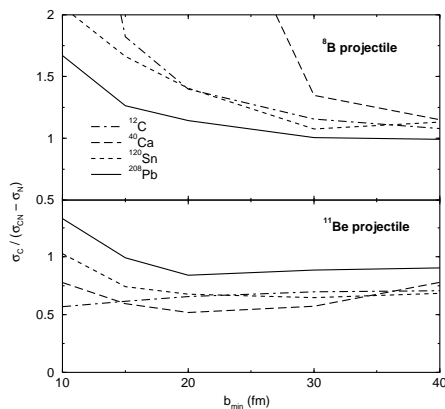


FIG. 5: Ratios of the true to the contaminated Coulomb breakup cross sections  $\sigma_C/\hat{\sigma}_C = \sigma_C/(\sigma_{CN} - \sigma_N)$  as a function of the lower radial cutoff  $b_{\min}$ , for four different targets. Results for  ${}^8\text{B}$  are shown in the upper panel, and for  ${}^{11}\text{Be}$  in the lower panel.

on the impact parameter restrictions, implemented by means of a maximum angle  $\theta_{\max}$  for integrating the cross sections over the centre of mass angle of the projectile fragments. By semiclassical theory, this angle is related to  $b_{\min}$  by  $\theta_{\max} = 2\eta/(kb_{\min})$ . We therefore use the same restrictions on the calculated breakup cross sections. In Fig. 5 we show the ratios of the ‘true’ to ‘contaminated’ Coulomb breakup cross sections  $\sigma_C/\hat{\sigma}_C = \sigma_C/(\sigma_{CN} - \sigma_N)$  as a function of the lower radial cutoff  $b_{\min}$ .

Ideally the ratios should be unity, but in fact we see that rarely do these values even *tend* to unity for large  $b_{\min}$ . Only for the  ${}^8\text{B}$  projectile on  ${}^{208}\text{Pb}$  does this occur, and the deviations from unity are worse in the  ${}^{11}\text{Be}$  case. These deviations from unity indicate either that the

long tail of the  ${}^{11}\text{Be}$  ground state wave function gives rise to small but significant deviations from the pure Coulomb results even at impact parameters  $\gtrsim 30$  fm, or that diffraction effects are large enough to break the semiclassical connection between  $b_{\min}$  and  $\theta_{\max}$ . Equivalent plots for the  ${}^7\text{Be}$  projectile (not shown) give ratios far from unity, from diffraction or refraction causing nuclear breakup fragments to come out at very forward angles, implying that there is no ‘safe’ angular region where Coulomb effects dominate [26]. In general, it is clear that theoretical breakup calculations of Coulomb-nuclear interference are needed for accurate results for the breakup of  ${}^{11}\text{Be}$  and  ${}^7\text{Be}$  on any target.

In conclusion, we have given evidence through detailed CDCC calculations of the scaling behaviour of the nuclear breakup cross-section. This cross-section does scale as  $A_T^{1/3}$ , the mass number of the target nucleus, but the scaling does not follow the geometrical form as in normal nuclei. The nuclear contribution can be as small as 1/15 of the values calculated in refs. [18, 19, 20]. We have further calculated the ‘error’ due to the nuclear-Coulomb interference in the extracted  $B(E1)$  distribution if the subtraction  $\sigma_{CN} - \sigma_N$  is employed in conjunction with the virtual photon method. We believe that a full quantum calculation, including both Coulomb and nuclear potentials on equal footing, such as CDCC, is required to get credible numbers for the  $B(E1)$  distribution of neutron- and proton-rich (as well as some stable) nuclei.

We acknowledge the support by the CNPq and FAPESP (Brazilian Agencies), by NSCL, Michigan State University, the National Science Foundation through grant PHY-0456656 and the U.K. EPSRC by grant GR/T28577.

- 
- [1] C. A. Bertulani and G. Baur, Phys. Rep. **163**, 299 (1988).  
[2] See, e.g. C. A. Bertulani, M. S. Hussein and G. Muenzenberg, ‘Physics of Radioactive Ion Beams’, Nova Science Publishing, 2001.  
[3] A. Winther and K. Alder, Nucl. Phys. **A319**, 518 (1979).  
[4] T. Nakamura, et al., Phys. Rev. Lett. **83**, 1112 (1999).  
[5] U. Datta Pramanik, et al., Phys. Lett. **B551**, 63 (2003).  
[6] N. Iwasa et. al., Phys. Rev. Lett. **83**, 2910(1999)  
[7] F. Schümann et. al., Phys. Rev. Lett. **90**, 232501(2003)  
[8] P. G. Hansen, A. S. Jensen, B. Jonson, Annu. Rev. Nucl. Part. Sci. **45**, 591 (1995)  
[9] I. Tanihata, Nucl. Phys. **A654**, 235c (1999).  
[10] T. Glasmacher, Annu. Rev. Nucl. Part. Sci. **48**, 1 (1998).  
[11] T. Aumann, et al. Phys. Rev. **C59**, 1252 (1999).  
[12] D. Sackett, et al. Phys. Rev. **C48**, 118 (1993).  
[13] F. Shimoura, et al., Phys. Lett. **B348**, 29 (1995).  
[14] M. Zinser, et al., Nucl. Phys. **A619**, 151 (1997).  
[15] T. Nakamura, et al., Phys. Lett. **B331**, 196 (1994).  
[16] A. Leistenschneider, et al., Phys. Rev. Lett. **86**, 5442 (2001).  
[17] T. Nakamura, Nucl. Phys. **A734**, 319 (2004).  
[18] C. H. Dasso, S. M. Lenzi and A. Vitturi, Nucl. Phys. **A639**, 635 (1998)  
[19] C. H. Dasso, S. M. Lenzi and A. Vitturi, Phys. Rev. **C59**, 539 (1999)  
[20] M. A. Nagarajan, C. H. Dasso, S. M. Lenzi and A. Vitturi, Phys. Lett. **B503**, 65 (2001)  
[21] R. Chatterjee and R. Shyam, Phys. Rev. **C66**, 061601(R) (2002).  
[22] S. Typel and R. Shyam, Phys. Rev. **C64**, 024605 (2001).  
[23] V. Maddalena and R. Shyam, **C63**, 051601 (2001).  
[24] I. J. Thompson, Comp. Phys. Repts. **7**, 167 (1988)  
[25] N. Austern et al. Phys. Rep. **154**, 125 (1987).  
[26] N.C. Summers and F.M. Nunes, Phys. Rev. **C70** 011602(R) (2004)  
[27] J. C. Acquadro, M. S. Hussein, D. Pereira and O. Sala, Phys. Lett. **B100**, 381 (1980)  
[28] R. Palit et al., Phys. Rev. C **68**, 034318 (2003).  
[29] T. Aumann, Eur. Phys. J. **A26**, 441 (2005).  
[30] N. Fukuda et al., Phys. Rev. **C70**, 054606 (2004).  
[31] K. Hencken, G. Bertsch and H. Esbensen, Phys. Rev. **C54**, 3043 (1996)

[32] T. Aumann, private communication.

[33] F. M. Nunes and I. J. Thompson, Phys. Rev. **C59**, 2652 (1999).

[34] J. A. Tostevin, F. M. Nunes and I. J. Thompson, Phys. Rev. **C63**, 024617 (2001).